Geochemical Fractionation between Porcellanite and Host Sediment

Masamichi Takebe and Koshi Yamamoto

Department of Earth and Planetary Sciences, Graduate School of Environmental Studies, Nagoya University, Chikusa, Nagoya 464-8602, Japan
(e-mail: takebe@gcl.eps.nagoya-u.ac.jp)

ABSTRACT

To reveal chemical fractionation during porcellanitization, we have examined chemical compositions of porcellanite clasts and their host sediments from DSDP sites 164 and 166. Porcellanite is an intermediate product during chert formation. Distinctly higher Si/Ti ratios are observed in porcellanite relative to the host sediment, indicating Si transfer from the host sediment. However, Ti-normalized values of Al, Fe, Mn, Ca, Na, K, P, rare earth elements, Sc, Rb, Y, Cs, Pb, Th, and Cr in porcellanite are similar to those of the host sediment, showing that these elements are affected by only very limited fractionation during porcellanitization and retain information about the sedimentary environment. The Si/Ti, P/Ti, and Al/Ti ratios in DSDP clayey samples fluctuate synchronously with their sedimentation ages. Because the Si/Ti and P/Ti ratios in clayey sediment reflect the contribution of biogenic siliceous and phosphatic debris, respectively, their high values in Cenozoic clayey sediments indicate vigorous biogenic productivity. Moreover, the observed similarity in age profiles of the Al/Ti ratio with the Si/Ti ratio and P/Ti ratio in clayey samples suggests that the Al/Ti ratio is affected by the supply of biogenic debris. The high Al/Ti ratios found in the Cenozoic samples can be ascribed to the contribution of adsorbed Al onto sinking biogenic debris. The small difference between the Al/Ti ratio of the Cenozoic porcellanite and the host sediment indicates that the adsorbed Al is also retained in porcellanite during Si enrichment. Therefore, the Al/Ti ratio in bedded cherts may be a potential indicator of ancient biogenic activity.

Introduction

Sediment cores sampled by the Deep Sea Drilling Project (DSDP) and Ocean Drilling Project (ODP) have been valuable sources of information for elucidating the evolutionary history of the earth's surface (cf. papers in Initial Reports of DSDP and Scientific Results of ODP). However, deep-sea sediments made accessible by such direct drilling are limited to those deposited in the post-Jurassic, because older oceanic crust has been subducted back into the earth. However, sedimentary rocks from the Precambrian to Recent can be found in accretionary complexes around the world. Thus, studies of accreted sedimentary rocks are indispensable for investigating the long-term history of the earth prior to the Cretaceous. Among the sedimentary rocks commonly found in accretionary complexes, bedded chert has a great potential for retrieving clues to long-term environmental fluctuations on the earth's surface. In comparison with other types of sedimentary rocks in accretional complexes, cherts have the following advantages for obtaining information on paleoenvironments: (1) long time span of sedimentation, (2) ease of age determination by radiolarians, and (3) high resistance to weathering. However, it should be noted that because of the extremely fine-grained character of detrital components, petrological information would be of little use in constraining the sedimentary conditions of a chert. Hence, geochemical approaches have commonly been employed to understand the depositional environments of cherts (Sugisaki et al. 1982; Murray et al. 1991, 1992*a*; Murray 1994; Yamamoto et al. 1997; Takayanagi 1998; Takayanagi et al. 2000).

Before we apply a geochemical method to earth surface processes, possible effects of elemental fractionation through diagenetic processes must be understood. In the case of cherts, the main diagenetic processes are successive dissolution-precipitation and recrystallization of silica during the transformation of opal-A into quartz through opal-CT

Manuscript received November 27, 2001; accepted September 19, 2002.

[The Journal of Geology, 2003, volume 111, p. 301–312] 0022-1376/2003/11103-0004$15.00

(Murata and Larson 1975; Pisciotto 1981). Regarding geochemical fractionation during the formation of chert, Murray et al. (1992*b*, 1992*c*) examined differences in chemical compositions between chert and host sediment during diagenesis. They targeted chert nodules occurring mainly in carbonate host sediments.

In contrast, in this study, we focus on porcellanites occurring in noncarbonate host sediments by examining DSDP 164 and 166 core samples containing porcellanite nodules. We compared the chemical composition of the porcellanite with that of the host sediment, which is composed mostly of pelagic clay and siliceous biogenic debris. This article addresses the elemental fractionation between porcellanite and the host sediment. Because porcellanite is the intermediate product between siliceous sediment and chert (Pisciotto 1981), this study focuses on the midpoint of chert formation.

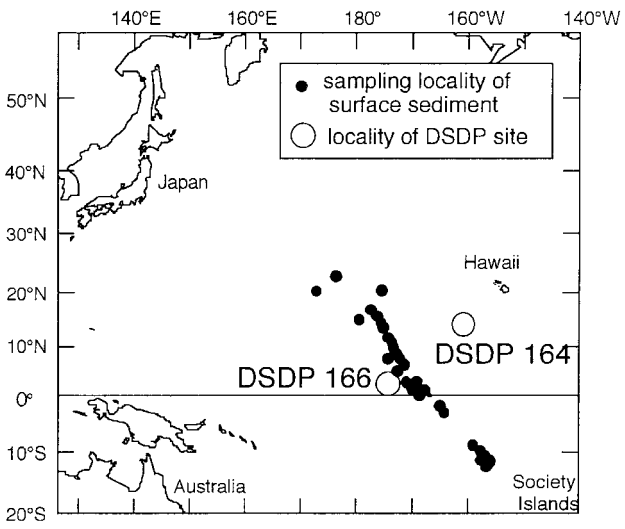

Figure 1. Location map of analyzed surface sediments and DSDP cores.

Sample and Method

Core samples from DSDP Sites 164 and 166 (open circles in fig. 1) were analyzed for major and trace elemental compositions. The sites are 5499 m and 6962 m below sea level and are deeper than the present calcite compensation depth (CCD). Analyzed samples are radiolarian oozes and pelagic clay, selected from the horizons shallower than 210 m below the sea floor (table 1; Shipboard Scientific Party 1973*a*, 1973*b*). Some samples contain porcellanites as clasts (table 1). Previously determined radiolarian ages of DSDP 164 and 166 samples are Cenomanian to Early Miocene and Eocene to Pliocene, respectively (table 1; Shipboard Scientific Party 1973*a*, 1973*b*). A hiatus between Cretaceous and Tertiary may be present in the DSDP 164 core (Shipboard Scientific Party 1973*a*). Porcellanites in the sample were handpicked from the host sediment, and only porcellanite samples with recovered weight >1 g were subjected for analysis.

Surface sediments around the equator are also analyzed for comparison (solid circles in fig. 1). In this article, box core samples and pilot core samples shallower than 30 cm from the core top are designated as "surface sediments." These samples were obtained during GH80-1, NH91-1, and NH93-1 research cruises by the Geological Survey of Japan and were recovered from water depths deeper than the CCD. $CaCO_3$ is therefore scarce in the samples. Samples yielding bubbles by addition of 1.7 M HCl were excluded because of the presence of the calcite.

Samples were prepared in the following way: NH91-1 and NH93-1 suites were dried in a vacuum chamber evacuated by a rotary pump and subsequently ground into less than 115 mesh. The DSDP 164 and 166 suites were rinsed with deionized water to remove salt, then dried at 110°C, and subsequently ground into less than 115 mesh. A GH80-1 suite was prepared by Sugisaki and Kinoshita (1982).

We analyzed 42 samples for major and rare earth elements (REEs) in this study. An additional 28 samples from GH80-1, whose major elemental data are available in Sugisaki and Kinoshita (1982) and are used in the following discussion, were also analyzed for REEs. We analyzed 39 DSDP samples for Co, Ni, Cu, Zn, Ga, Rb, Y, Zr, Mo, Cs, Ba, Pb, and Th. We also analyzed 12 porcellanites and six host sediments for Sc, Cr, and U.

XRF. Concentrations of major elements were determined by x-ray fluorescence (XRF) techniques on fused glass beads, prepared by fusing 0.7-g samples with 6.0 g lithium tetraborate. Calibration curves were obtained according to the method of Sugisaki et al. (1977), with standard rock samples issued from the Geological Survey of Japan. The XRF analyses were performed with a Shimadzu SXF-1200 equipped with a Rh x-ray tube (40 kV, 70 mA) at Nagoya University. Analytical precision was estimated to be >1% for Si and 3% for other elements, except for Ti, whose analytical precision is >3% when the measured Ti level is <0.1%. Ti concentrations of DSDP samples were also determined by inductively coupled plasma mass spectrometry (ICP-MS).

ICP-MS. REEs, Ti, Co, Ni, Cu, Zn, Ga, Rb, Y,

Table 1. Description of DSDP Samples from Sites 164 and 166

Sample name	Site	Depth (m)	Age	Classification	Porcellanite color	Luster
1C	164	20	Early Miocene	Clay	...	...
2C	164	36	Early Oligocene	Clay	...	...
3C	164	37	Early Oligocene	Clay	...	...
4C	164	44	Middle Eocene	Clay	...	...
4Poch	164	44	Middle Eocene	Porcellanite	Flesh	Bright
4Pocl	164	44	Middle Eocene	Porcellanite	Pale green	Dull
5C	164	62	Early Eocene	Clay	...	...
5Poch	164	62	Early Eocene	Porcellanite	Dark brown	Bright
5Pwcl	164	62	Early Eocene	Porcellanite	White	Dull
6C	164	76	Campanian	Clay	...	...
7C	164	80	Campanian	Clay	...	...
8C	164	103	Coniacian–Santonian	Clay	...	...
9C	164	105	Coniacian–Santonian	Clay	...	...
10C	164	110	Coniacian–Santonian	Clay	...	...
11C	164	118	Coniacian–Santonian	Clay	...	...
12C	164	124	Coniacian–Santonian	Clay	...	...
12Pfch	164	124	Coniacian–Santonian	Porcellanite	Flesh	Bright
13C	164	136	Coniacian–Santonian	Clay	...	...
13PfchA	164	136	Coniacian–Santonian	Porcellanite	Dark brown	Bright
13PgchB	164	136	Coniacian–Santonian	Porcellanite	Dark brown	Dull
14C	164	146	Coniacian–Santonian	Clay	...	...
15C	164	165	Cenomanian–Turonian	Clay	...	...
16C	164	182	Cenomanian–Turonian	Clay	...	...
17C	164	202	...	Clay	...	...
18C	166	3	Pliocene	Clay	...	...
19C	166	14	Late Miocene	Clay	...	...
20C	166	22	Middle Miocene	Clay	...	...
21C	166	87	Early Miocene	Clay	...	...
22C	166	124	Late Oligocene	Clay	...	...
23C	166	172	Late Eocene	Clay	...	...
24C	166	192	Middle Eocene	Clay	...	...
25C	166	195	Middle Eocene	Clay	...	...
26C	166	195	Middle Eocene	Clay	...	...
26Pwcl	166	195	Middle Eocene	Porcellanite	White	Dull
27Poch	166	198	...	Porcellanite	Dark brown	Bright
28C	166	198	...	Clay	...	...
31Pfch	166	205	...	Porcellanite	Flesh	Bright
31Poch	166	205	...	Porcellanite	Dark brown	Bright
31Pocl	166	205	...	Porcellanite	Dark brown	Dull

Zr, Mo, Cs, Ba, Pb, and Th were determined by ICP-MS with an HP4500 at Nagoya University. For REE determination, about 50 mg of sample were digested with 0.5 mL $HClO_4$ and 1 mL HF on a hot plate at 180°C and were subsequently dissolved in 1.7 M HCl. Sample solution was separated from the residue by centrifuge at 12,000 rpm. The residue was again digested with a 0.5-mL mixture of $HClO_4$ and HF on the hot plate at 180°C. The digested residue was dissolved in 1.7 M HCl, and the solution was again separated from residue by centrifuge. The remaining residue was fused with Na_2CO_3 and dissolved in 1.7 M HCl. All of the 1.7 M HCl solutions were mixed, dried on the hot plate, and redissolved in 2 mL of 1.7 M HCl. This sample solution was subjected to cation chromatographic separation (Dowex 50WX8) of REEs from major elements and Ba, which interfere with the REE analysis by ICP-MS. Finally, the sample solution was dissolved in 2% HNO_3 for ICP-MS analyses.

For determination of concentrations of Ti and trace elements other than REEs, 30-mg samples were digested with $HClO_4$ and HF in the same manner as for REE determination. The supernatant by centrifugation was dried on a hot plate and dissolved in 2% HNO_3 for ICP-MS analyses.

Mixed standard solutions made from individual REE oxides were used as external calibration standards for REE analyses. As external calibration standards of Ti, commercially available 1000 ppm standard solution was diluted with 2% HNO_3. Standard solutions for trace elements other than REEs were made from a standard composite glass prepared by Yamamoto and Morishita (1997) for trace element determinations by XRF. The pow-

dered standard glass (40 mg) was digested with 0.5 mL $HClO_4$ and 1 mL HF and diluted with 2% HNO_3. Indium was employed as an elemental internal standard for the determinations of Ti, Co, Ni, Cu, Zn, Ga, Rb, Y, Zr, Mo, Cs, and Ba, while Bi was employed for those of Pb and Th. In the REE analysis, both In and Bi were used for internal standards. Total blanks for Ti and REEs were not corrected because of their negligible contribution (<1%). Total blanks for most trace elements were <3%, and those of Zr and Pb were occasionally up to 10%. Appropriate blank corrections have been made for those elements. Analytical errors were estimated to be <3% for Ti, Rb, Pb, and REEs; <5% for Ga, Y, Ba, Cu, and Zn; <7% for Co, Ni, Zr, and Mo; and <10% for Cs and Th.

INAA. Co, Sc, Cr, Th, and U were determined by instrumental neutron activation analysis (INAA) for 12 porcellanites and six host sediments. Samples of about 100 mg and JB-1a as a standard were packed into separate ethylene bags. The bags were irradiated at the Japan Atomic Energy Research Institute with a thermal neutron flux of 5.5×10^{13} cm^{-2} s^{-1} for 5 min. Irradiated samples and standards were analyzed with a Ge semiconducting detector Seiko EG&G activation analysis system at the Radioisotope Center at Nagoya University. Analytical precision was >2%, 3%, 6%, 22%, and 28% for Co, Sc, Th, Cr, and U, respectively.

The major element and trace element concentrations were recalculated on the free basis of ignition loss (the complete data set is available from *The Journal of Geology* upon request). These recalculated concentrations are used in the following discussion and do not affect relative elemental abundance because all elements in the sample are corrected by the same factor.

Results and Discussion

Surface Sediment. The SiO_2 content of the surface sediment reaches the maximum value of up to 70 wt% around the equatorial Pacific and reaches the minimum value of <55 wt% around the Society Islands (15°S). The main sources of Si in marine sediments are detrital materials and biogenic opal, while Ti originates mainly from detrital materials (e.g., Sugisaki 1984; Murray and Leinen 1993). Therefore, the Si/Ti ratio can be an indicator of the relative contribution of biogenic debris to detrital materials. The distribution of Si/Ti ratios for the present samples is shown in figure 2. The Si/Ti ratios of the sediments around the equatorial region appear to have relatively higher values of

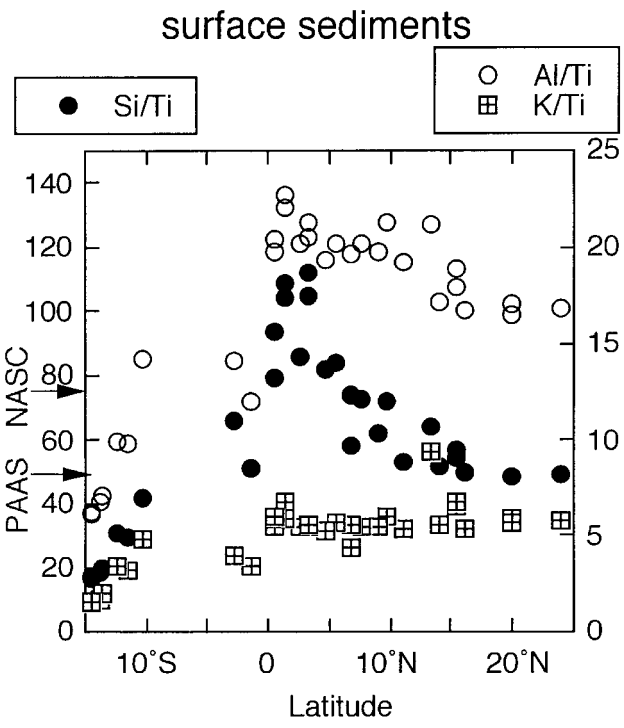

Figure 2. Latitudinal profiles of Ti-normalized values of Si, Al, and K in equatorial surface sediments.

80–110, whereas those around the Society Islands show low values of <20. Consistently low Al/Ti and K/Ti ratios are characteristic of a high Ti value for the Society Islands samples. We interpret this effect as a contribution of basaltic detritus with high Ti content at 15°S (cf. Murray and Leinen 1993, 1996), since the basalts that formed the Society Islands are characterized by relatively higher concentrations of Ti (2.0–4.0 wt%; Kogiso et al. 1997) than those of post-Archean Australian shale (PAAS; Taylor and McLennan 1985) and North American shale composite (NASC; Gromet et al 1984) with 1.0 wt% and 0.7 wt% of Ti, respectively.

In contrast to the Si/Ti ratios, the K/Ti ratios of surface sediments showed little variation irrespective of their sampling latitudes from 25°N to the equator. This suggests that variation of the Si/Ti ratios in the equatorial region is not due to the compositional difference of detrital materials. In the equatorial Pacific region, biological activity is so vigorous (Leinen 1992) that the chemical composition of the sediments would be affected largely by that of the biogenic opal (Leinen et al. 1986). Because the biogenic opal is composed mostly of SiO_2, a dominant contribution of opal should result in lower concentrations of elements other than Si in the sediments (Sugisaki and Kinoshita 1982; Ya-

mamoto 1983). Therefore, the observed high Si/Ti ratios in the equatorial sediments should reflect a large contribution of biogenic opal.

A latitudinal profile of Al/Ti ratios in the surface sediments parallels that of the Si/Ti ratios, and the highest value was also observed at an equatorial region (fig. 2). Thus, the variation in the Al/Ti ratios is probably related to the content of biogenic debris, as was inferred for the Si/Ti ratios. Murray et al. (1993) and Murray and Leinen (1996) reported that the Al/Ti ratios of equatorial sediments correlate with the bulk accumulation rate and model flux of ^{234}Th from seawater. Dymond et al. (1997) reported that biogenic opal is a predominant carrier of Al from seawater to sediment and suggested the possibility that the Al/Ti ratio can be used as a proxy for biogenic opal flux and/or the concentration of dissolved Al in seawater. These reports suggest that the variation of Al/Ti ratios shown in figure 2 probably reflects the contribution of Al adsorbed on biogenic debris from seawater.

DSDP Samples. *Comparison between porcellanite and host sediment.* Radiolarian shells filled with opal-CT were observed in thin sections of porcellanites in this study. This is consistent with the theory of Murray et al. (1992*c*) that the precipitation of SiO_2 is an important process for the formation of chert. The precipitation of SiO_2 derived from the host sediment results in the dilution of other elements in porcellanite and chert. Therefore, geochemical fractionation during porcellanite and chert formation should be recorded as elemental ratios of an objective element to a conservative one in porcellanite and chert and in the host sediment (Murray et al. 1992*b*, 1992*c*). In the following discussion, we use Ti as the normalizing element because of its conservative nature.

Figure 3 shows ratios of elements in porcellanite to host sediment normalized with respect to Ti concentrations (i.e., $[X/Ti]_{porcellanite}/[X/Ti]_{host\ sediment}$). Because the associated host sediments were not available for some porcellanites (27Poch, 31Poch, 31Pocl, and 31Pfch), their chemical compositions are compared with that of 28C host sediment, sampled at the nearest horizon to these porcellanites. However, the Fe/Ti ratio of 28C is exceptionally high (85.6) compared with other sediments (14.9 ± 3.3). Hence, 27Poch, 31Poch, 31Pocl, and 31Pfch show large deviations from unity in figure 3. These large deviations are probably caused by the distinctive nature of 28C and do not reflect chemical fractionation during porcellanitization. This is shown in figure 4*A* and 4*B*, in which the fractionation factors of those porcellanites are calculated with respect to the composition of 26C.

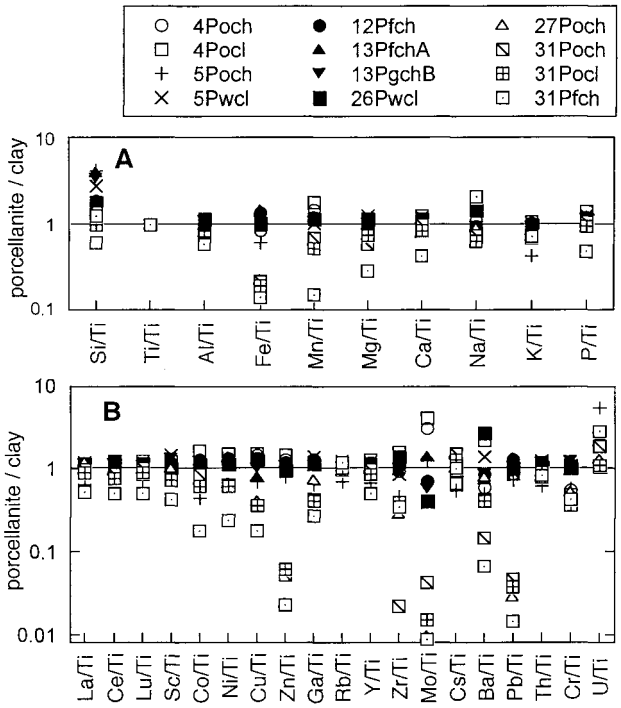

Figure 3. Ratios of Ti-normalized concentrations in porcellanite to those in host sediment. *A*, Major elements. *B*, Trace elements. Composition of 28C was used as the host sediment for 27Poch, 31Poch, 31Pocl, and 31Pfch.

Note that sample 26C was from the horizon second closest to those porcellanites and that the 26C-normalized fractionation factors of those porcellanites (27Poch, 31Poch, 31Pocl, and 31Pfch) are closer to unity, especially for Fe, Zn, Mo, Ba, Pb, and Cr.

In figure 4*A* and 4*B*, 31Pfch alone displays lower Ti-normalized values for elements other than Si, Na, K, Rb, Cs, Th, Cr, and U relative to those of 26C. Such deviations were not found in 31Poch and 31Pocl, which had been handpicked from the same sample as 31Pfch, indicating the possibility that 31Pfch has experienced some chemical processes that are independent from porcellanitization. Ti-normalized elemental ratios of cherts to host sediments from DSDP and the Monterey Formation by Murray et al. (1992*b*) are also shown in figure 4*C*.

As shown in figure 4*A* and 4*C*, the Ti-normalized Si contents of both porcellanite and chert are higher than those of the host sediment, implying that the porcellanitized part has a high SiO_2 content relative to host sediment. The higher SiO_2 reflects either a relatively high content of siliceous biogenic debris

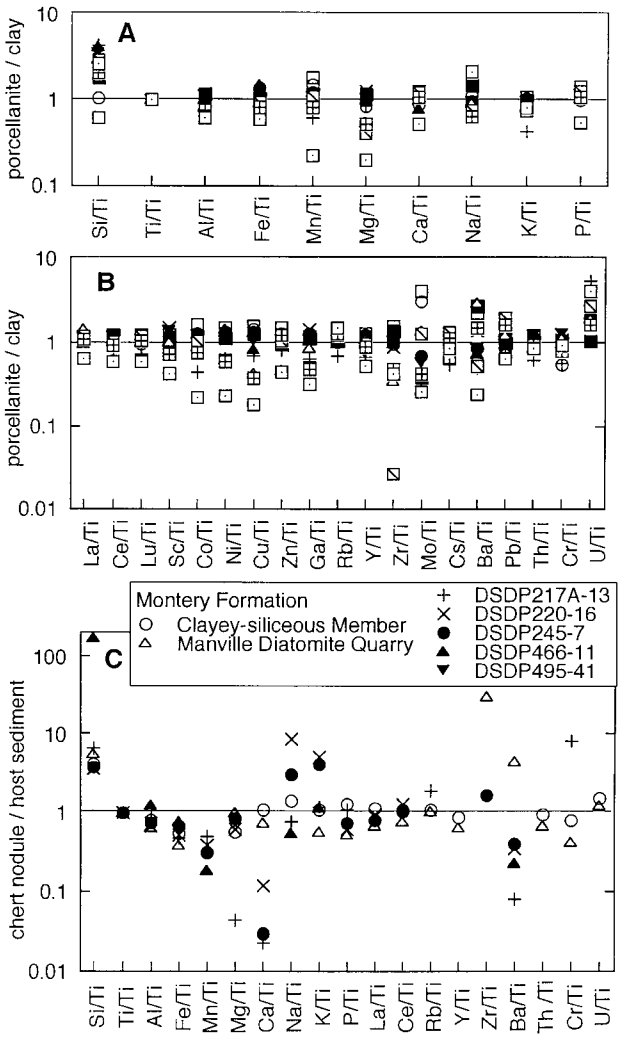

Figure 4. Ratios of Ti-normalized concentrations in porcellanite and chert to those of their host sediment. Composition of 26C was used as host sediment for 27Poch, 31Poch, 31Pocl, and 31Pfch. Symbols used in *A* and *B* are the same as those in figure 3. *A*, Major elements. *B*, Trace elements. *C*, Major and trace elements for DSDP samples and Monterey Formation samples reported by Murray et al. (1992*b*).

compared to the host sediment or diagenetic Si accumulation from the host sediment in an open system. The latter explanation is plausible because (1) porcellanites contain siliceous test cemented with opal-CT, and (2) there is little difference of P/Ti ratio between porcellanite and host sediment, implying similar contributions of biogenic debris and detrital materials, as discussed below. This interpretation of porcellanite formation is in agreement with Murray et al. (1992*b*). Another distinct feature of the porcellanites is the noticeable enrichment of U compared to the host sediment (fig. 4*B*). Because the U content of sediment depends largely on the redox condition (Calvert and Pedersen 1993), porcellanite formation might involve changes in the ambient redox condition.

On the basis of the above arguments, elements that appeared not to be fractionated during porcellanite formation are Al, Fe, Mn, Ca, Na, K, P, La, Ce, Lu, Sc, Rb, Y, Cs, Pb, Th, and Cr (see fig. 4*A* and 4*B* for their Ti-normalized ratios of about 1). However, Murray et al. (1992*b*) report some of these elements, such as Mg, Ca, Na, K, Ba, and Cr (see fig. 4*C*), were fractionated in DSDP samples during chert formation. In addition, Ti-normalized values of Fe and Mn in the chert nodule were reported to be lower than those of the host sediments (fig. 4*C*). Murray et al. (1992*b*) ascribed the low Mn/Ti ratios to preferential Mn loss during chert nodule formation. This idea was then generalized by Murray (1994) to a model that Mn was lost from silicified sediment during lenticular and bedded chert formation. The samples examined by Murray et al. (1992*b*) were DSDP chert nodules from carbonate host sediments, and the sediments from the Monterey Formation examined by Murray et al. (1992*b*) also contained carbonates. The porcellanites used in our work occur in silicate host sediments. Thus, some of the contradictions between the work of Murray et al. (1992*b*) and ours might be related to the difference in compositions of host sediments. For instance, the precipitation of $MnCO_3$ may be more feasible in carbonate sediment than in silicate sediment because the concentration of (Mn^{2+}) and (CO_3^{2-}) in pore water controls the precipitation of $MnCO_3$ (Okita 1992; Okita and Shanks 1992) and higher (CO_3^{2-}) concentration is expected in the pore water of carbonate sediment. In fact, Jones et al. (1994) reported that diagenetically altered Ca-carbonate tests have a relatively high Mn content. This may be the reason why the carbonate host sediments contain more Mn compared to the chert clasts. In this respect, these low Ti-normalized values of Mn in the chert nodules relative to those in the carbonate host sediments might not directly reflect the fractionation during porcellanitization. This further suggests that the application of the Murray (1994) model might be limited to the formation of cherts in carbonate host sediments and that the apparently fractionated Fe, Mg, Ca, Na, K, Ba, and Cr contents might reflect the chemical fractionation related particularly to the carbonate host sediments. Because the porcellanites in the present study are contained in silicate sediment, the results of this study can provide more reliable information about the chemical fractionation during the dia-

genesis of bedded cherts associated with silicate shale partings. Unlike the cherts in carbonate hosts, there is no evidence for significant elemental fractionation of Fe, Mn, Mg, Ca, Na, K, and Cr during porcellanitization in silicate sediments.

REE characteristics. The sedimentary environments of DSDP sites 164 and 166 can be envisaged on the basis of Ti-normalized values of Al, P, REEs, Rb, and Th, which are conservative elements during porcellanitization. Si/Ti ratios of the DSDP samples except for porcellanites are also useful indicators of the contribution of biogenic opal. Examples of REE patterns of the DSDP samples are shown in figure 5*A* and 5*B*. The La concentrations range from a few ppm to 150 ppm and Lu varies from 0.1 ppm to 3 ppm. The REE patterns of the DSDP samples are less variable and can be classified into two groups: (1) those with progressive and moderate depletion from La to Lu and (2) those with progressive enrichment from La to Gd and no apparent fractionation for heavier elements. Most of the Upper Cretaceous samples have the former (depleted REE composition), while post-Cretaceous samples fall into the latter group. All DSDP samples show negative Ce anomalies, which tend to be more negative for samples with relatively enriched heavy REEs. Only the oldest sample (17C) shows a positive Eu anomaly and enrichment of heavy REE relative to light REE (fig. 5*A*, 5*B*). For comparison, figure 5*C* shows REE patterns of Chinese loess reported by Liu et al. (1993) and Gallet et al. (1996) and biogenic apatite estimated by Takebe (2001). The REE patterns of 1 and 2 resemble those of the loess and biogenic apatite, respectively.

Detrital component. Figure 6 shows the correlation diagrams of Rb/Ti versus Th/Ti, Al/Ti versus Th/Ti, and Al/Ti versus K/Ti. These ratios are expected to provide clues to infer the source of the detrital component in the DSDP samples because K, Th, Rb, and Ti in sediment are believed to originate from the detrital component (Kyte et al. 1993). With respect to K/Ti, Th/Ti, and Rb/Ti ratios, most DSDP 164 and 166 samples have ratios close to the NASC and PAAS, suggesting that the detrital component in DSDP samples is mostly derived from the continental crust (fig. 6). In addition, in most cases, the small variations of K/Ti, Th/Ti, and Rb/Ti ratios indicate little contribution of other detrital materials to the sediments in DSDP 164 and 166 during the Late Cretaceous to present. In contrast, four samples with clearly smaller Th/Ti ratios (5Poch, 17C, 22C, and 23C) must contain detrital materials derived from other sources. In fact, Th/Ti ratios from Hawaiian basalts (Garcia et al. 1993) or andesites (Condie 1993) are significantly smaller than those of NASC and PAAS, indicating the likelihood of their involvement in formation of these four samples. The apparent occurrence in 17C of a positive Eu anomaly with

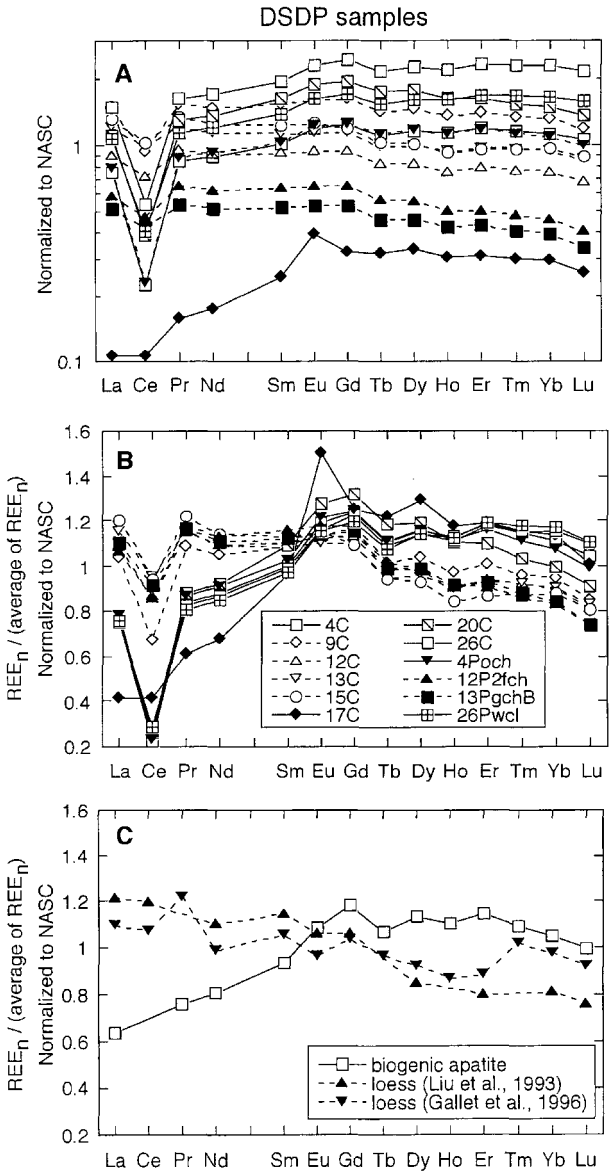

Figure 5. Examples of REE patterns of DSDP 164 and 166 samples normalized to NASC (Gromet et al. 1984) modified by Kawabe et al. (1998). *A*, NASC-normalized REE patterns. Key to symbols is shown in *B*. *B*, NASC-normalized patterns in which averages of the normalized values of each REE were adjusted to be unity to remove the effect of variation in REE concentrations. *C*, NASC-normalized patterns of Chinese loess (Liu et al. 1993; Gallet et al. 1996) and estimated biogenic apatite (Takebe 2001). The averages of the normalized values of each REE were also adjusted to unity.

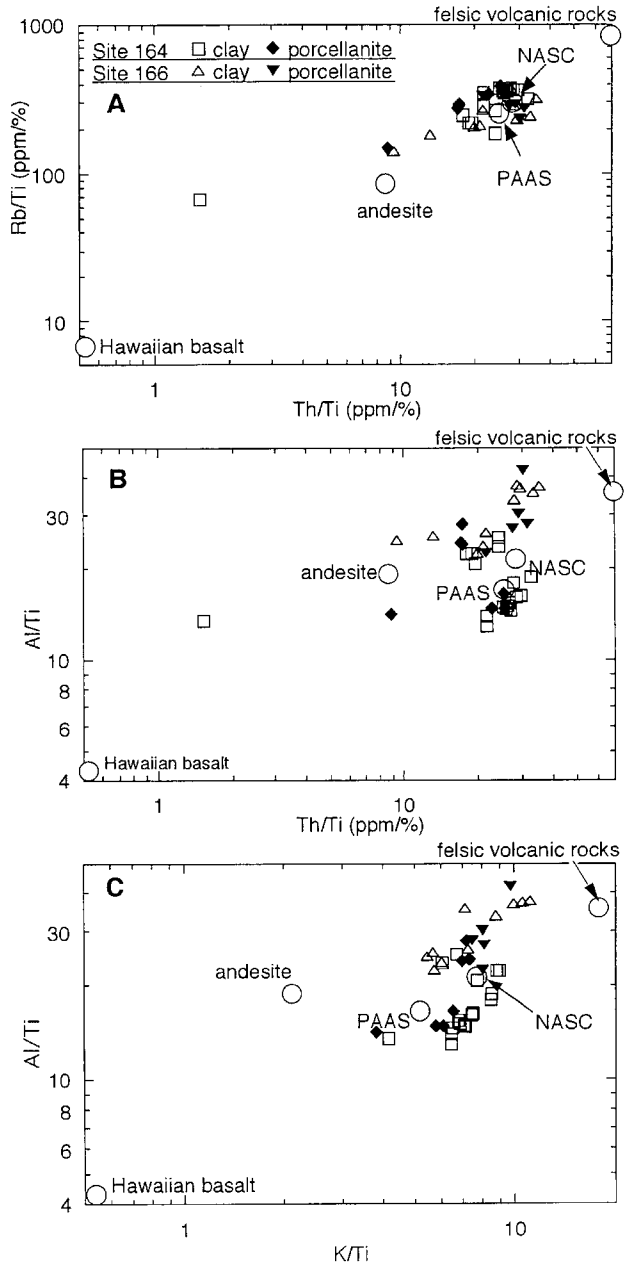

Figure 6. Ti-normalized values of some elements in DSDP samples. *A*, Rb/Ti (ppm/%) versus Th/Ti (ppm/%) ratios. *B*, Al/Ti versus Th/Ti (ppm/%) ratios. *C*, Al/Ti versus K/Ti ratios. The data for PAAS, NASC, and Hawaiian basalt are from Taylor and McLennan (1985), Gromet et al. (1984), and Garcia et al. (1993), respectively. The data for andesite and felsic volcanic rocks are from Condie (1993).

the smallest Th/Ti ratio is also consistent with the geochemical characteristics of oceanic island basalt (Garcia et al. 1993). Hence, sample 17C probably contains basaltic detritus derived from oceanic islands.

Biogenic production: Si/Ti ratio. To discuss the contribution of biogenic Si to sediments and the relation between Si/Ti ratio and biogenic debris, this section focuses only on clayey samples, which are considered to be free from diagenetic Si enrichment. The volume of porcellanites is so small relative to that of the clayey host sediment that Si enrichment of porcellanites has not greatly affected the host sediment's Si content. Strictly speaking, Si/Ti ratios of the host sediments containing porcellanites show the lower limits of the original Si/Ti ratios at deposition. The Si/Ti ratios of clayey sediments including host sediment are plotted against their respective ages in figure 7*A*, together with those for porcellanites for reference. The range of ratios of surface sediments from the equator to 20°N is indicated by the solid bar at the top of each figure (fig. 7). The Si/Ti ratios of the Upper Cretaceous samples are within the range reported for the surface sediments (Si/Ti = 16.5–112.1). The Eocene samples show remarkably higher Si/Ti ratios, some of which are >1000, even for the clayey samples. The post-Eocene samples from DSDP 166 also have higher Si/Ti ratios than those of the surface sediments.

In the study area, the chemical compositions of detrital materials show little variation through the depositional age, except for a few samples. Thus, the Si/Ti ratio in the clayey sediments should reflect a contribution of biogenic opal relative to detrital materials. The Upper Cretaceous clayey samples have Si/Ti ratios similar to those of PAAS and NASC, suggesting a very limited contribution, if any, of biogenic opal to bulk accumulation in DSDP 164 during the Late Cretaceous. In contrast, higher Si/Ti ratios of Eocene clayey samples suggest rapid accumulation of biogenic opal relative to terrestrial material.

Biogenic production: P/Ti ratio. Figure 7*B* shows the age profile of the P/Ti ratios of the DSDP samples. There is a clear cutoff in P/Ti ratios between the Upper Cretaceous and post-Cretaceous samples. The P/Ti ratios of the Upper Cretaceous samples are similar to those of PAAS and NASC and increase with age. In the Cenozoic samples, the P/Ti ratios exhibit the maximum value of about 6 in the Eocene and decrease with age to 1.5.

The P/Ti ratios of DSDP samples show a strong positive correlation with Ca/Ti ratios, except for some samples with anomalously high Ca/Ti ratios ($R = 0.995$; fig. 8). In figure 8*A*, part 2, the slope of the correlation agrees very well with the Ca/P ratio defined by the ideal chemical composition

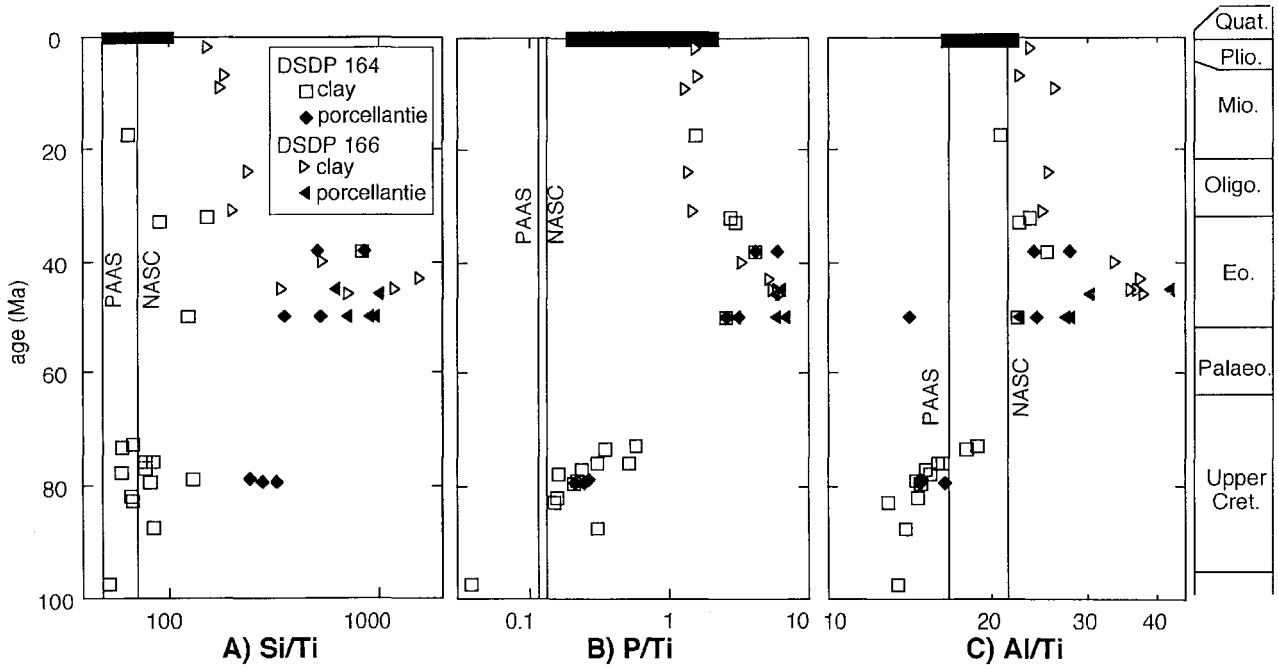

Figure 7. Age profile of Ti-normalized values in DSDP 164 and 166 samples. *A*, Si/Ti; *B*, P/Ti; *C*, Al/Ti ratios. A solid bar at the top of each diagram indicates range of the ratios in the surface sediments from the equator to 20°N. The data for PAAS and NASC are from Taylor and McLennan (1985) and Gromet et al. (1984), respectively. Geological time scale is that defined by Odin (1994). *Quat.* = Quaternary, *Plio.* = Pliocene, *Mio.* = Miocene, *Oligo.* = Oligocene, *Eo.* = Eocene, *Palaeo.* = Paleocene, *Upper Cret.* = Upper Cretaceous.

of carbonate-fluor-apatite (CFA; $Ca_5[PO_4]_{2.6}[CO_3]_{0.4}$ [OH, F, Cl]), strongly indicating that P and Ca in the DSDP samples are associated with the CFA.

The major candidates for CFA in pelagic sediment are fish debris and authigenic minerals. Toyoda et al. (1990) reported relatively high P concentration and abundant fish debris in the 2–100-μm-grained fraction of the surface pelagic sediments from the east equatorial Pacific. This observation indicates the important role of fish debris as a source of P in the pelagic sediments. In various Pacific regions, the fish debris is reported to be largely concentrated in Upper Paleogene to Lower Eocene sediments (Doyle and Riedel 1979, 1980, 1981; Winfrey et al. 1987). The DSDP samples in this study also have the highest P/Ti ratio in the Eocene samples. In addition, the P/Ti ratios of the DSDP clayey samples correlate with their Si/Ti ratios, which are indices of biogenic debris (fig. 7*A*, 7*B*). Thus, we regard the main source of P in the DSDP samples as likely to be fish debris. Although the possible presence of diagenetic apatite was previously reported (Filippelli and Delaney 1996), we note that its contribution to the total P budget should be quite limited because P/Ti ratios of the DSDP samples do not show any correlation with either the sedimentation depth or the degree of porcellanitization.

As shown in figure 8*B*, P/Ti ratios in DSDP samples show a strong positive correlation with REE/Ti ratios. Since P is mainly contained as biogenic apatite in those samples, REEs also seem to be contained in the biogenic apatite. Takebe (2001) reported the same correlation between P and REE for Pacific surface sediments and calculated the REE composition of biogenic apatite on the basis of the correlation (fig. 5*C*). The Eocene DSDP samples in this study show a similar REE pattern to that estimated for the apatite by Takebe (2001). Therefore, the REE composition of the Eocene samples are also likely to be significantly affected by biogenic apatite. Toyoda and Tokonami (1990) proposed that biogenic apatite can concentrate REEs from seawater and/or pore water after sedimentation.

As discussed above, P and REEs are conservative during porcellanitization. Therefore, the contents of P and REEs in a porcellanite can be indicators of paleoproductivity.

Adsorbed Al and porcellanitization. The temporal variations of Al/Ti ratios in the DSDP sam-

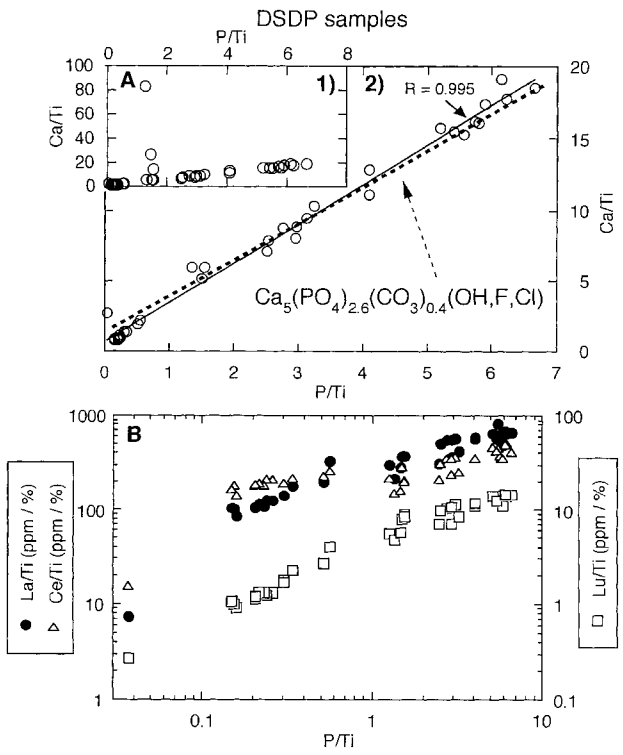

Figure 8. *A*, Ti-normalized values of Ca and P in DSDP 164 and 166 samples. *A-1* for DSDP samples and *A-2* for sediments, except for samples with exceptionally high Ca/Ti ratios. Solid and broken lines indicate the regression line for the present samples and ratio of Ca to P in an ideal CFA $Ca_5(PO_4)_{2.6}(CO_3)_{0.4}$(OH, F, Cl), respectively. *B*, Relationships between Ti-normalized values of REEs (La, Ce, and Lu) and P in DSDP 164 and 166 samples.

ples follow a path similar to that observed for P/Ti ratios (fig. 7*B* and 7*C*). The Al/Ti ratios of the Upper Cretaceous samples increase with age. Most Cenozoic samples have higher Al/Ti ratios than those in the surface sediments. The Al/Ti ratios of the Eocene samples are particularly high, >30 in some cases. One sample, 5Poch, has an exceptionally low Al/Ti ratio compared with other Eocene samples. It should be noted that 5Poch also has Th/Ti and Rb/Ti ratios clearly distinct from those of NASC and PAAS.

Sugisaki et al. (1982) pointed out that Al and Ti in sediment are derived largely from detrital components. Despite the large and uniform contribution of terrigenous material from the Upper Cretaceous to the present as shown in figure 6, the Al/Ti ratios fluctuate greatly with age. Al/Ti ratios of some Eocene DSDP 166 samples are extremely higher than those of PAAS and NASC. Moreover, figure 6*B* and 6*C* indicates that the Al enrichment is not associated with fluctuation of K, Th, Rb, and Ti contents, which depends largely on chemical composition of detrital materials. Consequently, Al can be regarded as originating partly from components other than detrital materials. The fluctuation of the Al/Ti ratio of DSDP samples against age is also synchronized not only to that of the P/Ti ratio but also to the Si/Ti ratio of the clayey samples. As discussed above, P/Ti and Si/Ti ratios are largely influenced by the contribution of biogenic debris. As shown clearly in figure 9, Al/Ti ratios are positively correlated with Si/Ti ratios for clayey samples with Si/Ti ratios >20. Therefore, the Al/Ti ratios of the DSDP samples are probably affected by biogenic productivity. Murray et al. (1993) and Murray and Leinen (1996) reported that Al/Ti ratio fluctuation in core samples at the equatorial Pacific is associated with glacial-interglacial cycles, indicating that the Al/Ti ratio can be a possible proxy for biogenic productivity for Quaternary samples. This result suggests a possibility that the Al/Ti ratio can also be used as the same proxy for older sediment to Cretaceous.

For the adaptation of the Al/Ti ratio in porcellanite and/or chert as a paleoproductivity index, fractionation of adsorbed Al during porcellanite and chert formation must be clarified. Although Al in aluminosilicate is considered to be conservative during diagenesis (Murray 1994), there has been no discussion as to whether adsorbed Al is conservative or not during the processes. The Cenozoic DSDP samples are inferred to contain large amounts of adsorbed Al. As discussed above, there is little difference of Al/Ti ratio between porcellanite and host sediment in the Cenozoic samples (fig. 4). This strongly suggests that the adsorbed Al

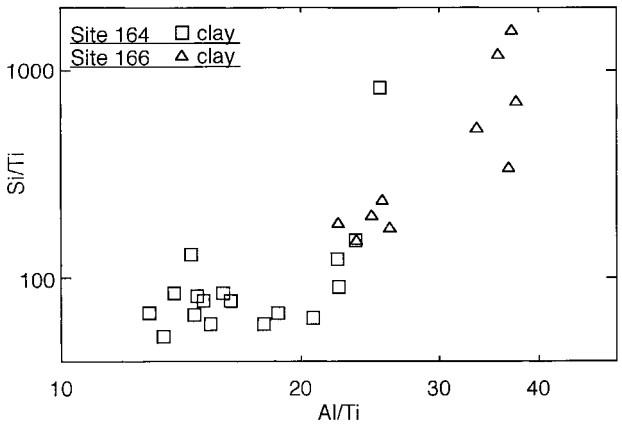

Figure 9. Ti-normalized values of Si and Al in DSDP clayey samples.

is conservative during porcellanitization and that the Al/Ti ratio in porcellanite and chert can be an indicator of the relative accumulation rate of biogenic debris to detrital materials.

Conclusion

We have analyzed major and trace elemental abundance in porcellanite clasts and their host sediments to explore the application of geochemical information to problems related to the formation of cherts. Porcellanite gains Si from host sediment in open system during porcellanitization. On the other hand, Al, Fe, Mn, Ca, Na, K, P, REEs, Sc, Rb, Y, Cs, Pb, and Th are considered to be conservative during porcellanitization. This suggests that such elements in the porcellanites preserve information on the sedimentary environment. In addition, this article shows that the Al/Ti ratio and the P/Ti ratio behave conservatively during porcellanitization and that both ratios can be potential indicators of paleoproductivity of marine biota.

ACKNOWLEDGMENTS

M. Kawate of the University of Tokyo and H. Kojima, T. Tanaka, and S. Shibata of the University of Nagoya assisted us in the INAA. We thank T. Matsumoto, University of Osaka, and also C. N. Richardson, University of Cambridge, for revising the English version of this article. J. Bode and J. Firth provided the DSDP samples. Our surface sediments were collected during GH80-1 cruises of the Geological Survey of Japan and NH91-1 and NH93-1 cruises of the Northwest Pacific Carbon Cycle Study, assigned to the Kansai Environmental Engineering Center by the New Energy and Industrial Technology Development Organization.

REFERENCES CITED

Calvert, S. E., and Pedersen, T. F. 1993. Geochemistry of recent oxic and anoxic marine sediments: implications for the geological record. Mar. Geol. 113:37–88.

Condie, K. C. 1993. Chemical composition and evolution of the upper continental crust: contrasting results from surface samples and shales. Chem. Geol. 104: 1–37.

Doyle, P. S., and Riedel, W. R. 1979. Cretaceous to Neogene ichthyoliths in a giant piston core from the central North Pacific. Micropaleontology 25:337–364.

———. 1980. Ichthyoliths from site 436, northwest Pacific, Deep Sea Drilling Project leg 56. *In* Lee, M., and Stout, L. N., eds. Initial reports of the Deep Sea Drilling Project, vols. 56 and 57, pt. 2, p. 887–893.

———. 1981. Ichthyoliths at site 464, northwest Pacific, Deep Sea Drilling Project leg 62. *In* Stout, L. N., ed. Initial reports of the Deep Sea Drilling Project 62: 491–494.

Dymond, J.; Collier, R.; McManus, J.; Honjo, S.; and Manganini, S. 1997. Can the aluminum and titanium contents of ocean sediments be used to determine the paleoproductivity of the oceans? Paleoceanography 12:586–593.

Filippelli, G. M., and Delaney, M. L. 1996. Phosphorous geochemistry of equatorial Pacific sediments. Geochim. Cosmochim. Acta 60:1479–1495.

Gallet, S.; Jahn, B.; and Torii, M. 1996. Geochemical characterization of the Luochuan loess-paleosol sequence, China, and paleoclimatic implications. Chem. Geol. 133:67–88.

Garcia, M. O.; Jorgenson, B. A.; Mahoney, J. J.; Ito, E; and Irving, A. J. 1993. An evaluation of temporal geochemical evolution of Loihi summit lavas: result from Alvin submersible dives. J. Geophys. Res. 98:573–550.

Gromet, L. P.; Dymek, R. F.; Haskin, L. A.; and Korotev, R. L. 1984. The "North American shale composite": its complication, major and trace element characteristics. Geochim. Cosmochim. Acta 48:2469–3482.

Jones, C. E.; Jenkyns, H. C.; and Hesselbo, S. P. 1994. Strontium isotopes in Early Jurassic seawater. Geochim. Cosmochim. Acta 58:1285–1301.

Kawabe, I.; Toriumi, T.; Ohta, A.; and Miura, N. 1998. Monoisotopic REE abundances in seawater and the origin of seawater tetrad effect. Geochem. J. 32: 213–229.

Kogiso, T.; Tatsumi, Y.; Shimoda, G.; and Barsczus, H. G. 1997. High μ (HIMU) ocean island basalts in southern Polynesia: new evidence for whole mantle scale recycling of subducted oceanic crust. J. Geophys. Res. 102:8085–8103.

Kyte, R. T.; Leinen, M.; Heath, G. R.; and Zhou, L. 1993. Cenozoic sedimentation history of the central North Pacific: inferences from the elemental geochemistry of core LL44-GPC3. Geochim. Cosmochim. Acta 57: 1719–1740.

Leinen, M. 1992. Biogenic silica. *In* Libes, S. M., ed. An introduction to marine biochemistry. New York, Wiley, p. 262–273.

Leinen, M.; Heath, G. R.; Biscaye, P. E.; Kolla, V.; Thiede, J.; and Dauphin, J. P. 1986. Distribution of biogenic silica and quartz in recent deep-sea sediments. Geology 14:199–203.

Liu, C.; Masuda, A.; Okada, A.; Yabuki, A.; Zhang, J.; and Fan, Z. 1993. A geochemical study of loess and desert sand in northern China: implications for continental crust weathering and composition. Chem. Geol. 106: 359–374.

Murata, K. J., and Larson, R. R. 1975. Diagenesis of Miocene siliceous shale, Temblor range, California. J. Res. U.S. Geol. Surv. 3:553–599.

Murray, R. W. 1994. Chemical criteria to identify the depositional environment of chert: general principles and applications. Sediment. Geol. 90:213–232.

Murray, R. W.; Buchholtzten Brink, M. R.; Gerlach, D. C.; Russ, G. P., III; and Jones, D. L. 1991. Rare earth, major, and trace elements in chert from the Franciscan Complex and Monterey Group, California: assessing REE sources to fine-grained marine sediments. Geochim. Cosmochim. Acta 55:1875–1895.

———. 1992*a*. Interoceanic variation in the rare earth, major, and trace element depositional chemistry of chert: perspectives gained from the DSDP and ODP record. Geochim. Cosmochim. Acta 56:1897–1913.

———. 1992*b*. Rare earth, major, and trace element composition of Monterey and DSDP chert and associated host sediment: assessing the influence of chemical fractionation during diagenesis. Geochim. Cosmochim. Acta 56:2657–2671.

Murray, R. W.; Jones, D. L.; and Buchholtzten Brink, M. R. 1992*c*. Diagenetic formation of bedded chert: evidence from chemistry of the chert-shale couplet. Geology 20:271–274.

Murray, R. W., and Leinen, M. 1993. Chemical transport to the equatorial Pacific Ocean across a latitudinal transect at 135°W: tracking sedimentary major, trace, and rare earth element fluxes at the equator and the Intertropical Convergence Zone. Geochim. Cosmochim. Acta 57:4141–4163.

———. 1996. Scavenged excess aluminum and its relationship to bulk titanium in biogenic sediment from the central equatorial Pacific Ocean. Geochim. Cosmochim. Acta 60:3869–3878.

Murray, R. W.; Leinen, M.; and Isern, A. R. 1993. The biogenic flux of Al to sediment in the equatorial Pacific Ocean: evidence for increased productivity during glacial periods. Paleoceanography 8:651–670.

Odin, G. S. 1994. Geological time scale (1994). Ser. II. C. R. Acad. Sci. Paris 318:59–71.

Okita, P. M. 1992. Manganese carbonate mineralization in the Monlango District, Mexico. Econ. Geol. 87: 1345–1366.

Okita, P. M., and Shanks, W. C., III. 1992. Origin of stratiform sediment-hosted manganese carbonate ore deposits: examples from Molango, Mexico, and Tao Jiang, China. Chem. Geol. 99:139–164.

Pisciotto, K. A. 1981. Diagenetic trends in the siliceous facies of the Monterey Shale in the Santa Maria region, California. Sedimentology 28:547–571.

Shipboard Scientific Party. 1973*a*. Site 164. *In* Roth, P. H., and Herring, J. R., eds. Initial reports of the Deep Sea Drilling Project 17:17–45.

———. 1973*b*. Site 166. *In* Roth, P. H., and Herring, J. R., eds. Initial reports of the Deep Sea Drilling Project 17:103–143.

Sugisaki, R. 1984. Relation between chemical composition and sedimentation rate of Pacific ocean-floor sediments deposited since the Middle Cretaceous: basic evidence for chemical constraints on depositional environment of ancient sediments. J. Geol. 92:235–259.

Sugisaki, R., and Kinoshita, T. 1982. Major element chemistry of the sediments on the central Pacific transect, Wake to Tahiti, GH80-1 cruise. *In* Mizuno, A., and Nakao, S., eds. Regional data of marine geology, geophysics, and manganese nodules: the Wake-Tahiti transect in the central Pacific. Geol. Surv. Jpn. Cruise Rep. 18:293–312.

Sugisaki, R.; Shimomura, T.; and Ando, K. 1977. An automatic x-ray fluorescence method for the analysis of silicate rocks. J. Geol. Soc. Jpn. 83:725–733.

Sugisaki, R.; Yamamoto, K.; and Adachi, M. 1982. Triassic bedded cherts in central Japan are not pelagic. Nature 298:644–647.

Takayanagi, Y. 1998. Depositional environments of bedded cherts of the Shimanto terrane, the Kii Peninsula, inferred from normal paraffin and major element compositions. J. Geol. Soc. Jpn. 104:501–515.

Takayanagi, Y.; Yamamoto, K.; Yogo, S.; and Adachi, M. 2000. Depositional environment of the Cretaceous Shimanto bedded chert from the Fukura area, Kochi Prefecture, inferred from major element, rare earth element and normal paraffin compositions. J. Geol. Soc. Jpn. 106:632–645.

Takebe, M. 2001. Rare earth element compositions of deep sea sediments from central to western Pacific: discussion about main factors controlling REE composition of marine sediments by factor analysis. J. Geol. Soc. Jpn. 107:301–315.

Taylor, S. R., and McLennan, S. M. 1985. The continental crust: its composition and evolution. London, Blackwell, 312 p.

Toyoda, K.; Nakamura, Y.; and Masuda, A. 1990. Rare earth elements of Pacific pelagic sediments. Geochim. Cosmochim. Acta 54:1093–1103.

Toyoda, K., and Tokonami, M. 1990. Diffusion of rare-earth elements in fish teeth from deep-sea sediments. Nature 345:607–609.

Winfrey, E. C.; Doyle, P. S.; and Riedel, W. R. 1987. Preliminary ichthyolith biostratigraphy, southwest Pacific, Deep Sea Drilling Project leg 91. *In* Menard, H. W.; Natland, J.; et al., eds. Initial reports of the Deep Sea Drilling Project 91:447–468.

Yamamoto, K. 1983. Geochemical study of Triassic bedded cherts from Kamiaso, Gifu Prefecture. J. Geol. Soc. Jpn. 89:143–162.

Yamamoto, K., and Morishita, T. 1997. Preparation of standard composites for the trace element analysis by x-ray fluorescence. J. Geol. Soc. Jpn. 103:1037–1045.

Yamamoto, K.; Nakamaru, K.; and Adachi, M. 1997. Depositional environments of "accreted bedded cherts" in the Shimanto terrane, Southwest Japan, on the basis of major and minor element compositions. J. Earth Planet. Sci. 44:1–19.